

Post-liquefaction Settlement Evaluation Method of Non-plastic Silty Sand

Mei Hsun Chang¹, Jing Wen Chen¹, and Wei Feng Lee²

¹Department of Civil Engineering, National Cheng Kung University, Tainan, Taiwan

²Ground Master Construction Co., LTD.

E-mail: anitachang224@gmail.com

ABSTRACT: Although the soil liquefaction potential has been the focus of considerable research, post-liquefaction subsidence has not yet received equal attention. In addition to this, non-plastic silty sand is observed in areas where severe earthquakes have occurred in Japan, Taiwan, and New Zealand, and thus the soil liquefaction engineering properties of such soil need to be investigated immediately. In the past five years, the authors applied the new sampling techniques to obtain high quality soil samples, and a series of soil tests were performed to determine the dynamic properties and post-liquefaction volumetric strain behaviours of non-plastic silty sand. In this study, the applicability of the current settlement evaluation methods in Taiwan is discussed based on relevant research results first. Then, for the convenience of use, the formulation of analysis process of the current evaluation methods is proposed. Finally, considering the influence of the volumetric strain behaviour of non-plastic silty sand, the modifications to current evaluation methods of the silty sand post-liquefaction settlement were then proposed using case verifications. It is considered that analysis results using the suggested modifications proposed in this study are more consistent than those of the previous methods.

KEYWORDS: Non-plastic silty sand, Post-liquefaction volumetric strain, Evaluation method.

1. INTRODUCTION

Although the soil liquefaction potential had been the focus of many studies, post-liquefaction secondary disasters have not attracted attention. However, many serious disasters have been caused by post-liquefaction subsidence. For example, a wide distribution of non-plastic silty sand lies in the areas where recent severe earthquakes have occurred in Japan, Taiwan, and New Zealand, and serious soil liquefaction damage was observed after the 1999 Chi-Chi earthquake in the central Taiwan in the Wu Feng, Nan Tou, and Yuen Lin areas. According to the post-earthquake study results, most soil liquefaction took place in silty sand deposits with high fines grade content, and this was also seen in areas damaged by the Christchurch earthquakes in 2010–2011. Non-plastic silty sand is recognized as the major source of soil liquefaction, and therefore it is necessary for researchers to consider the serious consequences that could affect infrastructure built on such soil.

Research has been conducted on the special soil liquefaction engineering properties of non-plastic silty sand and excellent results have been obtained. The engineering properties of this soil have been extensively investigated with respect to the soil liquefaction induced ground failure. However, in the past five decades, although research on the influence of the fine content and particle properties on the soil liquefaction potential has been proposed by many researchers, test results have only been focused on the influence of plastic fine particles of remolded soil specimens, and due to the limitations of non-plastic silty sand sampling technology, the effect of the silty sand particle structure (deposition conditions and void ratio) and the non-plastic fines content have not yet been determined. Recently, a research team comprising the authors of this paper and Prof. Ishihara successfully applied the Gel-Push sampler to obtain undisturbed specimens in the Tainan-Hsinhua area of liquefaction; soil dynamic tests of undisturbed non-plastic silty sand were conducted and related research results were successively published in 2011.

Non-plastic silty sand with high fines content (SM or ML with $PI < 4$) extensively covers areas in the central to southern parts of the western Taiwan. Regional soil liquefaction damage occurred in silty sand deposits during the Chi-Chi earthquake and in a series of earthquakes occurring between 2010 and 2011. Although current evaluation methods for soil liquefaction potential and post-liquefaction volumetric strain have been developed, they have focused only on clean sand, and soil fine aggregates have only been considered with respect to the plastic fines content or soil plasticity index. However, non-plastic fines can affect the soil structure and

cause incorrect evaluation results, and therefore, the current methods of evaluation are inappropriate for use in areas of silty sand with a non-plastic fines content of more than 10%.

Prior to an earthquake, the deposition state of a saturated loose sand layer is loosely arranged. When an earthquake occurs, strong cyclic loading results in a rise in soil pore water pressure and a reduction in soil effective pressure until liquefaction occurs. Following an earthquake, there is a dissipation of excess pore water pressure, and the density of the soil structure increases. Therefore, post-liquefaction, volumetric strain causes ground-surface subsidence phenomena. The ground surface settlement is related to the volume of water drained (Glaser, 1993; Ishihara, 1993); this phenomenon is similar to that of the consolidation settlement of the clay layer and is known as post-liquefaction settlement.

Lee & Albaisa (1974) investigated the post-liquefaction volumetric strain behavior of Monterey sand using cyclic triaxial tests. Their results indicated that the influential factors in volumetric strain include relative density, particle size, and initial effective confining pressure. Tatsuoka et al. (1984) concluded that post-liquefaction volumetric strain is primarily affected by maximum shear strain, γ_{max} , followed by the relative density, and that the effect related to the initially effective confining pressure is small. Tokimatsu & Seed (1987) based their study on that of Tatsuoka et al. (1984) and proposed a relation between post-liquefaction volumetric strain (ϵ), cyclic stress ratio, and the corrected standard penetration test value (N_{160}). The relation between maximum shear strain and the post-liquefaction volumetric strain was proposed by Nagase & Ishihara (1988), who defined that initial liquefaction occurs when the maximum shear strain of the sand layer achieves 3.5%.

Additionally, Ishihara & Yoshimine (1992) performed laboratory shear tests (a direct shear test, triaxial test, and a torsional shear test) using Fujikawa clean sand specimens. They proposed a relationship between maximum shear strain and post-liquefaction volumetric strain under different relative density conditions, and also developed an assessment curve for the post-liquefaction volumetric strain with an associated analytical method. Yamamuro & Lade (1997, 1998) and Lade & Yamamuro (1997) indicated that the volumetric compressibility increases with an increase in the non-plastic fines content. Tsukamoto et al. (2004) conducted tests on post-liquefaction volumetric strain with clean sand and soil with fines ($F_c = 0\%–43.3\%$) and proposed relative assessment curves and an associated analytical processes for Toyoura sand ($F_c = 0\%$). Ishihara et al. (2016) used dynamic test results conducted on non-plastic silty sand (Tainan Hsinhua and Bengal Padma) to determine

the post-liquefaction volumetric strain (ϵ_{vmax}) of undisturbed and remolded specimens, and additionally proposed a relationship between relative density (D_r) and post-liquefaction volumetric strain (ϵ_{vmax}). A list of studies conducted on the post-liquefaction volumetric strain of silty sand is shown in Figure 1. From these studies, the post-liquefaction volumetric strain (settlement) evaluation methods proposed by Ishihara & Yoshimine (1992) and Tsukamoto et al. (2004) are the most commonly used methods. For the convenience of use, the formulation of analysis process of the current evaluation methods is proposed in the proposed study. Modifications were made to the method used to evaluate the post-liquefaction settlement of silty sand, according to the above assessment method principles, and results are verified using case examples.

Time	Researcher	Test equipment or analysis method	Test sand
1970	1971 Silver & Seed	Simple shear test	Monterey sand
	1974 Lee & Albaisa	Triaxial test	
1980	1984 Tatsuoka et al.	Simple shear, Torsional shear	Sengenyama sand
	1987 Tokimatsu & Seed	Simplified analysis method	Sengenyama sand
	1988 Nagase & Ishihara	Simple shear test	Fuji river sand
1990	1992 Ishihara & Yoshimine	Simple shear, Torsional shear, Triaxial test	Fujikawa clean sand
	1992 Ishihara & Yoshimine	Assessment method	Fujikawa clean sand
	1993 Lin & Chen	Triaxial test	Clean sand, Silty sand
	1997 Lade & Yamamuro	Triaxial test	Nevada sand
	1997 Ji	Formulation of assessment method	Kaohsiung sand
	1997 Ji	Formulation of assessment method	Fujikawa clean sand
	1998 Yamamuro & Lade	Triaxial test	Nevada sand
2000	2004 Tsukamoto et al.	Assessment method	Clean sand, Silty sand
	2004 Ko	Triaxial test	Mailiao sand
	2007 Yu	Triaxial test	Kaohsiung sand
2010	2016 Ishihara et al.	Assessment method	Clean sand, Silty sand

Figure 1 Research time table of post-liquefaction volumetric strain of silty sand

2. SOIL LIQUEFACTION PROPERTIES OF NON-PLASTIC SILTY SAND

The Hsinhwa area (HH01) is located in the south Tainan and consists of interbedding between a non-plastic silty sand layer and a non-plastic clay layer. Severe soil liquefaction occurred in this area in relation to the JiaSian earthquake in 2010, and this area of soil liquefaction has since become a major research site. In the past researches, the area of damage situated close to the Taiwan high speed rail was selected to investigate the post-liquefaction volumetric strain behavior of non-plastic silty sand. Soil dynamic triaxial tests were conducted on undisturbed specimens of non-plastic silty sand obtained using a Gel-Push (GP) sampler and comparative remolded specimens (Chen et al., 2014; Lee et al., 2015). The influence of void ratio, fines content, and the disturbance effect on the post-liquefaction volumetric strain behavior of non-plastic silty sand was determined using the methods of Tsukamoto et al. (2004) and Chen et al. (2014) (Chang et al., 2017).

The study site, Hsinhwa City, Tainan, Taiwan, was selected because of an existing widespread soil liquefaction that occurred in relation to an earthquake of magnitude 6.4 in 2010. Figure 2 summarizes the soil profile at the test site, and as shown in the figure, a silty sand layer was selected for analysis that is located between 3 and 10 m below the ground's surface has a high fines content ranging from 10% to more than 50% (Lee et al., 2015).

A total of four boreholes were drilled; GP sampling was conducted in three boreholes, and conventional Shelby tube sampling was conducted in the fourth hole for comparison purposes. The soil type of HH01 specimens is classified as SM or ML using the USCS system. In accordance with the easy liquefied grain size distribution curve of the Japan Society of Civil Engineers, the specimens are classed as belonging to the soil with a high liquefaction potential. The site moisture content (ω) of this soil type

is higher than the liquid limit and the fines particles are non-plastic; these results indicate that HH01 specimens are extremely sensitive to disturbance effects. Non-plastic silty sand particles are small (and are non-plastic). Therefore, a weakening phenomenon occurs easily in its natural structure under disturbance effects. Due to the limitations of sampling techniques, although the dynamic engineering properties of non-plastic silty sand have been investigated in past research, the results obtained have been based on the use of remolded specimens because of the difficulty in obtaining high quality undisturbed soil specimens.

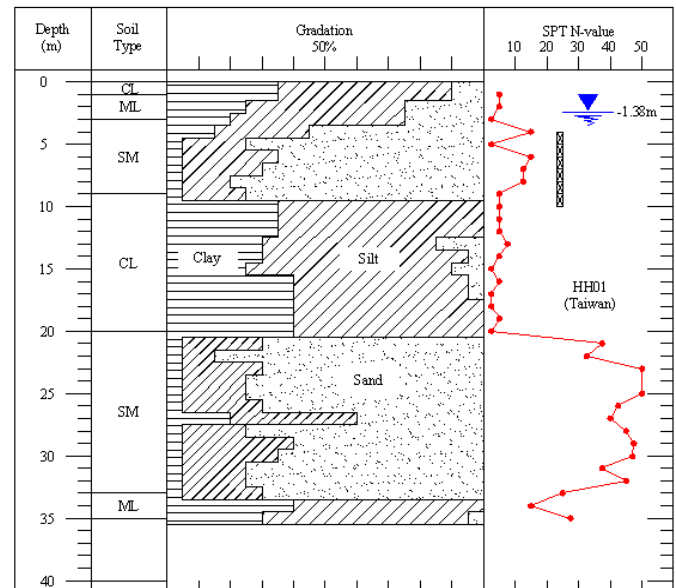


Figure 2 Soil profile at Hsinhwa area

To solve this difficulty related to the traditional sampling techniques used with sensitive non-plastic silty sand, the Gel-Push sampling technique (GP sampler) was developed by Kiso-Jiban Consultants Co. Ltd. and authors in 2006 (Figure 3 shows sampler parts). This sampler is designed to allow polymer lubricant to seep into the tube wall when the tube penetrates into the soil under hydraulic pressure. The polymer gel effectively reduces wall friction to allow recovery of a good quality sensitive silty sand specimen. The sampler is also designed with a cutter attached to the guiding tube to allow smooth penetration, and a catcher fixed at bottom of the thin wall tube holds the soil specimen to prevent it from falling out during the uplift. In the present study, this type of high quality undisturbed non-plastic silty sand specimen sampler was used in follow up tests conducted indoors.

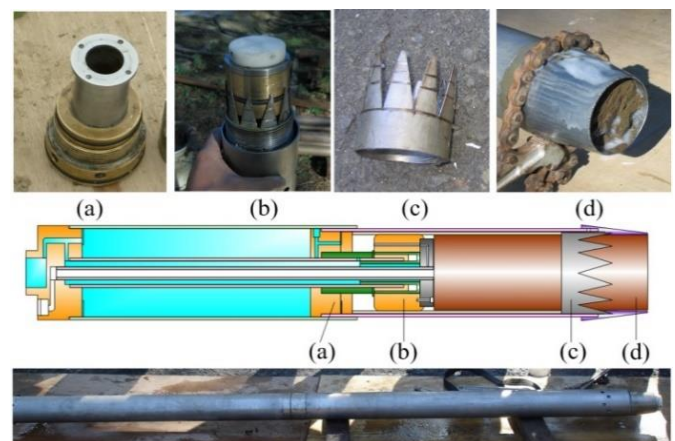


Figure 3 The configuration of the Gel-Push sampler

The cyclic triaxial testing apparatus proposed by C. K. Chan is used for this study. In the tests, soil liquefaction failure is related to

an effective stress failure and axial strain failure. Effective stress failure occurs when excess pore water pressure is equal to the total stress and the effective stress approaches zero; initial liquefaction occurs at this point. Axial strain failure represents ignition of liquefaction set as double amplitude (DA), $DA = 2X_0$, where X_0 is the single amplitude of axial strain exceeding 5%. Tests were terminated when either one of the failure types occurred. The initial test conditions were then restored and the below drainage gate was opened to dissipate pore water pressure. When pore water pressure was equal to zero, the amount of water discharged and the maximum axial strain was recorded to calculate the post-liquefaction volumetric strain (ϵ_v) and maximum shear strain (γ_{max}).

In an earlier study, the authors determined the dynamic engineering properties of non-plastic silty sand and presented dynamic characteristics and a pore water pressure duration curve; these results are shown in Figure 4 (Lee et al., 2015). Using an identical test state, the soil liquefaction resistance of undisturbed non-plastic silty sand specimens obtained with the GP sampler was found to be higher than that of remolded specimens, and undisturbed soil specimens withstood higher cyclic shear stress and numbers of cycles.

The influence of void ratio, fines content and the disturbance effect on the post-liquefaction volumetric strain behavior of non-plastic silty sand was determined based on the results provided in Tsukamoto et al. (2004) and Chen et al. (2014).

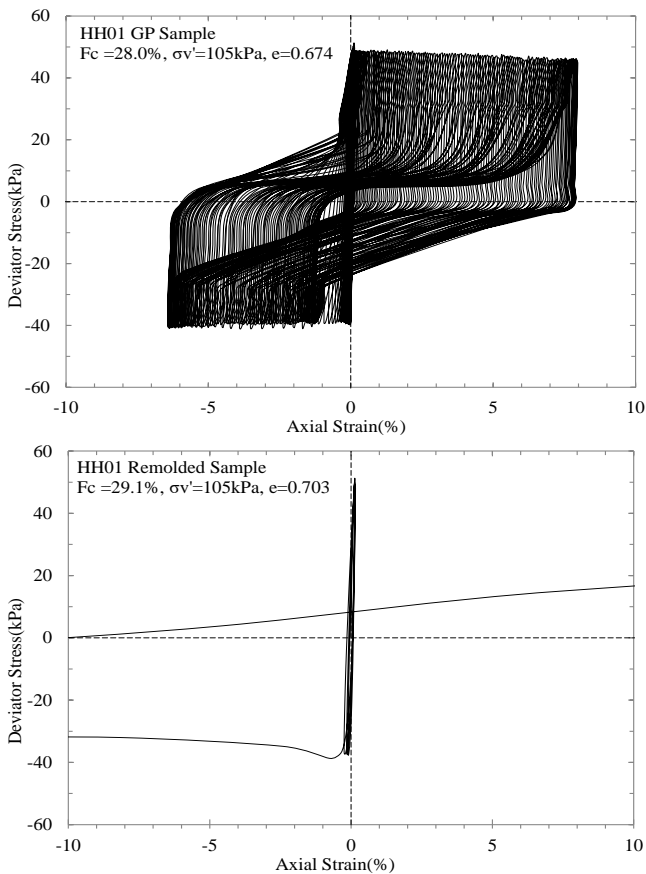


Figure 4 Typical results of cyclic triaxial tests. (Lee et al., 2015)

A series of remolded soil specimens were adopted to investigate the influence of the void ratio on the post-liquefaction volumetric strain behavior of non-plastic silty sand. As shown in Figure 5, ϵ_v is plotted against γ_{max} for remolded non-plastic silty sand and Toyoura sand, which is standard clean sand in Japan. It is important to note here that values of ϵ_v become greater with an increase in the value of γ_{max} , and values tend to stay constant at γ_{max} values higher than about 8%–10%, which can be referred to as the point of maximum post-liquefaction volumetric strain, ϵ_{vmax} . Moreover, ϵ_v values of non-plastic silty sand remolded samples were found to be

considerably higher than those of Toyoura sand, and ϵ_{vmax} increased with an increase in the void ratio. Figure 6 shows a plot of ϵ_v values against γ_{max} values for an undisturbed non-plastic silty sand and Toyoura sand, where it can be seen that for the non-plastic silty sand undisturbed soil sample, ϵ_v values increase with an increase in γ_{max} and tend to remain constant at γ_{max} values higher than about 14%–16%. As shown in Figures 5 and 6, the ϵ_v value of the undisturbed soil specimen was smaller than that of the remolded one under the same test conditions, but both were considerably greater than that of Toyoura sand. In addition, when the void ratio and relative density of the test specimens were similar, the post-liquefaction volumetric strain increased with an increase in the fines content. A comparison of the test results for undisturbed and remolded specimens under identical test boundary conditions shows the influence of the disturbance effect on post-liquefaction volumetric strain behavior. Figure 7 shows that the post-liquefaction volumetric strain increases with an increase in the maximum shear strain. When the test statuses of the soil specimens were similar, the post-liquefaction volumetric strain of undisturbed specimens was evidently lower than that of remolded specimens (Chang et al., 2017).

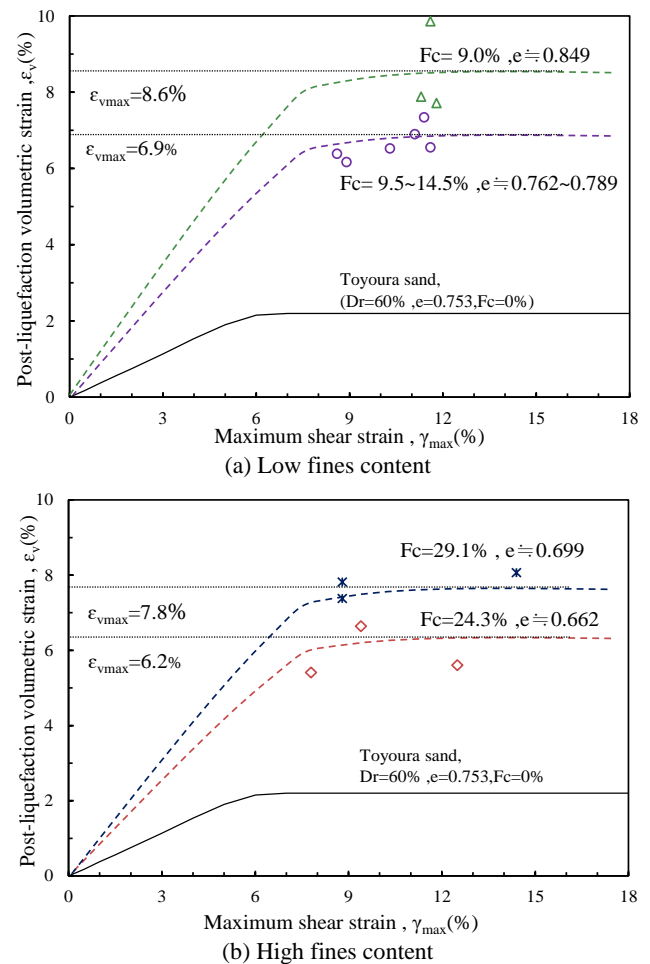


Figure 5 The influence of void ratio to post-liquefaction volumetric strain of Hsinhwa remolded specimens.

3. CURRENT POST-LIQUEFACTION SETTLEMENT EVALUATION METHOD

3.1 Current evaluation methods

Ishihara & Yoshimine (1992) performed laboratory shear tests (a direct shear test, triaxial test, and a torsional shear test) using Fujikawa clean sand specimens. They proposed a relationship between maximum shear strain, post-liquefaction volumetric strain and factor of safety against liquefaction (F_L) under different relative density conditions, as shown in Figure 8, and also developed an assessment curve for the post-liquefaction volumetric strain with an

associated analytical method. The results of the research indicate that when the maximum shear strain is small, it is approximately linear with post-liquefaction volumetric strain. When the shear strain gradually increases to a certain value (about 8%), the post-liquefaction volumetric strain remains unchanged and no longer changes with the maximum shear strain. The post-liquefaction volumetric strain decreased with relative density increased. One approach was proposed by Ishihara & Yoshimine in 1992, and chart formulation of this post-liquefaction settlement evaluation method was presented by Chi & Ou (2005) (hereinafter referred to as I&Y1992).

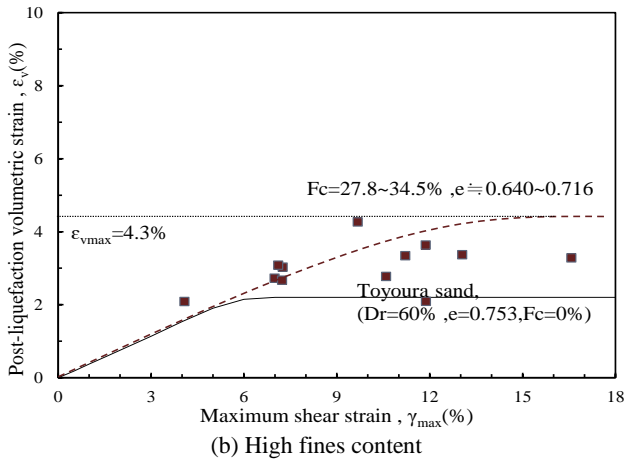
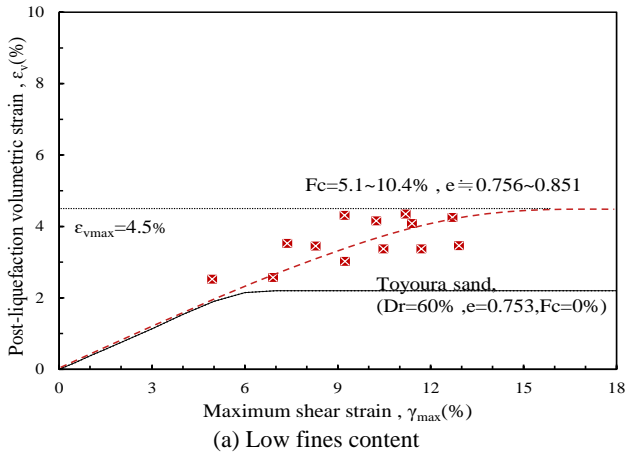


Figure 6 The influence of fines content to post-liquefaction volumetric strain of Hsinhwa remolded specimens.

Tsukamoto et al.(2004) used the cyclic triaxial extension and compression test to collect test results of post-liquefaction volumetric strain for clean sand and fine-grained soils ($F_c=0\sim43.3\%$). It showed that when the soil was subjected to a cyclic shear stress, the maximum shear strain, γ_{max} , increases with the increase of CSR. When the CSR continues to increase to a certain value, this value is approximately equal to CSR_{20} , and γ_{max} approaches a limit value. In the relationship between the maximum shear strain and the liquefaction factor of safety (F_L), when the soil is subjected to a cyclic shear stress, the maximum shear strain increases with the decrease of the liquefaction factor of safety. When F_L approaches 1 or less than 1, γ_{max} will reach the limit. In the relationship of maximum shear strain and post-liquefaction volumetric strain, the post-liquefaction volumetric strain increases with the increase of the maximum shear strain. When the shear stress rises to a certain value, the post-liquefaction volumetric strain will tend to be fixed. Combining the above research results, the relationship between post-liquefaction volumetric strain and liquefaction factor of safety can be obtained, and then post-liquefaction volumetric strain of each stage can be normalized. The post-liquefaction volumetric strain evaluation curve of fine-grained soil was obtained as shown in

Figure 9, and the relative evaluation procedure was proposed at the same time (hereinafter referred to as T.I.&S.2004).

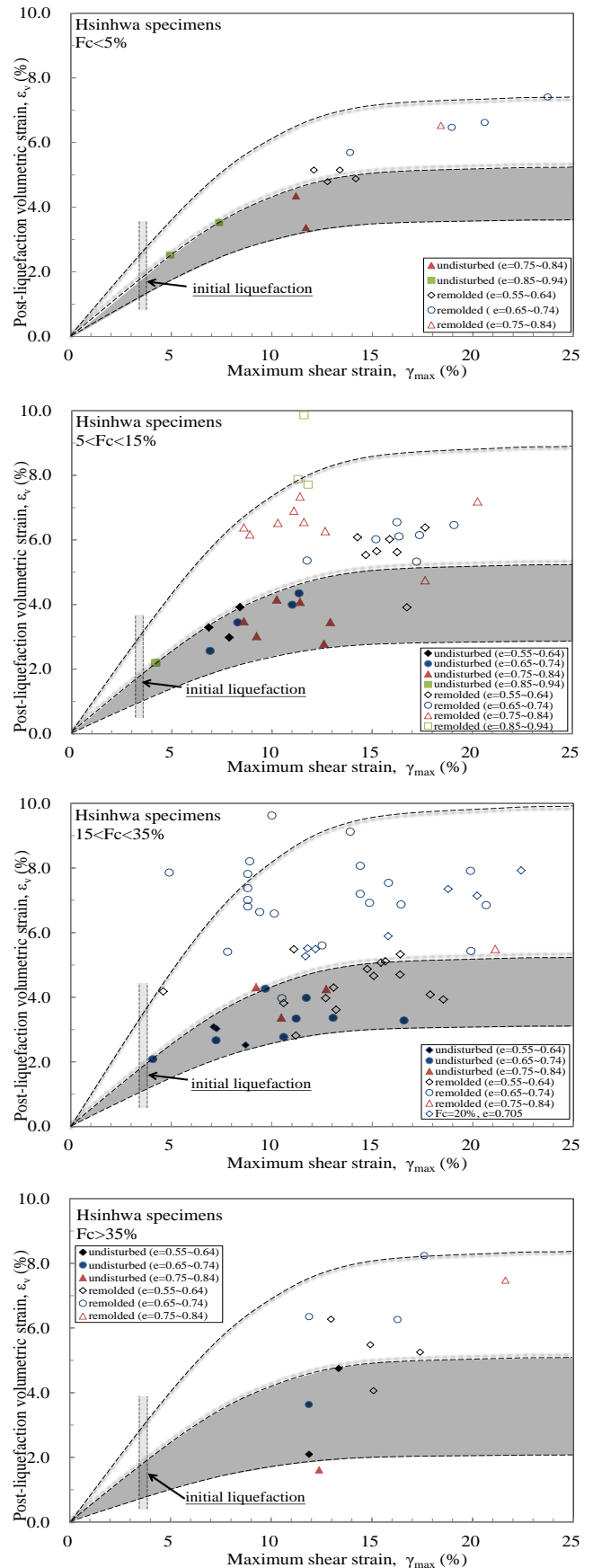


Figure 7 The influence of disturbance effect to post-liquefaction volumetric strain of Hsinhwa specimens.

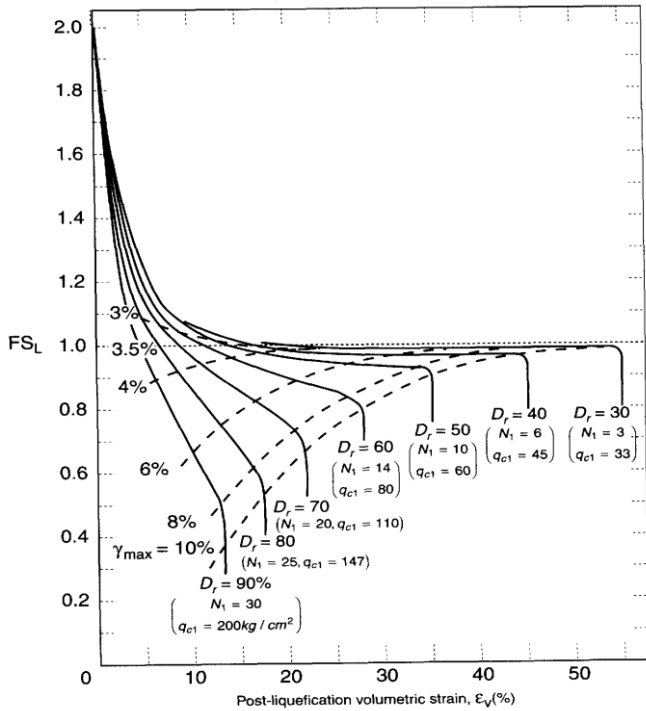


Figure 8 The relationship between post-liquefaction volumetric strain and factor of safety against liquefaction (Ishihara & Yoshimine, 1992)

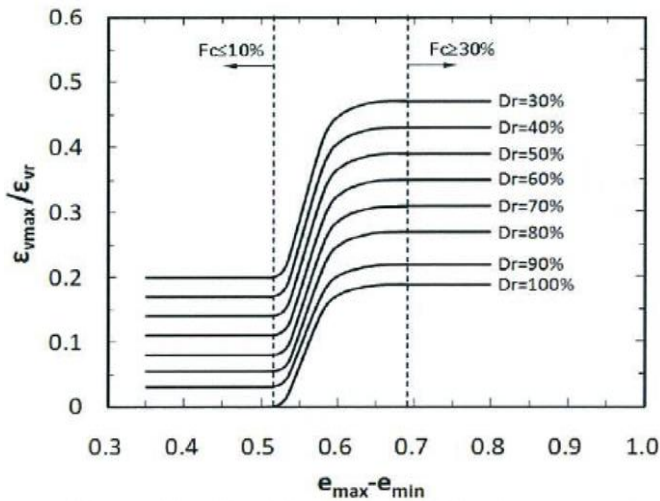


Figure 9 Post-liquefaction volumetric strain evaluation curve of fine-grained soil (Tsukamoto et al., 2004)

Ishihara et al. (2016) collected dynamic test results for non-plastic Taiwan Hsinhwa and Bengal Padma silty sand to determine the post-liquefaction volumetric strain (ϵ_{vmax}) of undisturbed and remolded specimens. The relationship between relative density (D_r) and post-liquefaction volumetric strain (ϵ_{vmax}) is shown in Figure 10 (Ishihara et al., 2016), where the scale of volumetric strain following the earthquake is classified using maximum shear strain. When maximum shear strain was equal to 10%, it was deemed to have the potential to cause maximum post-liquefaction volumetric strain in soils of natural alluvial deposits. This research indicated that there was a decrease in post-liquefaction volumetric strain with an increase in relative density, and the effect of the existence of soil fine aggregates on post-liquefaction volumetric strain of remolded specimens was significantly greater than that of undisturbed specimens. Based on the above results, another post-liquefaction settlement evaluation method was proposed by Ishihara et al. in 2016.

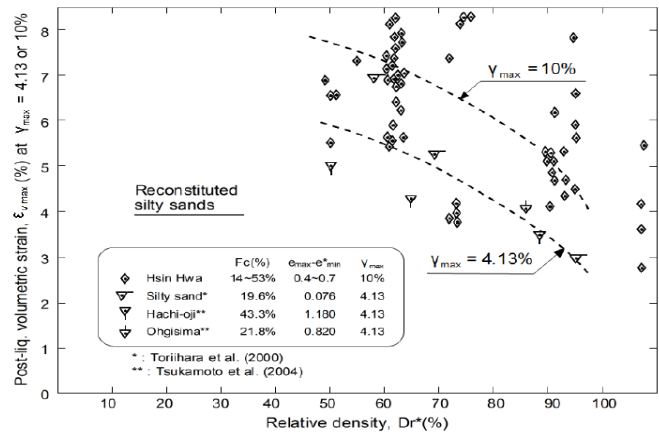
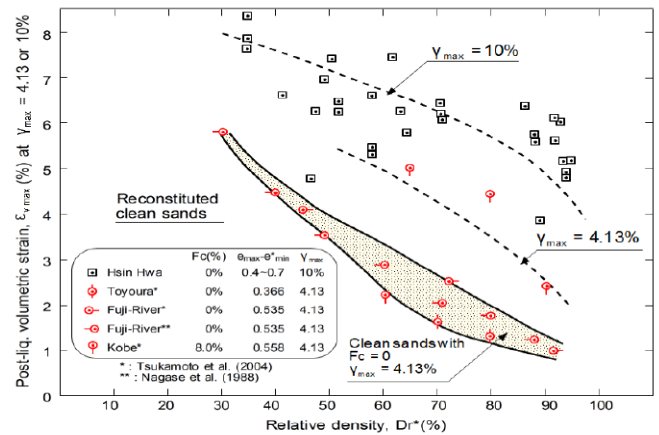
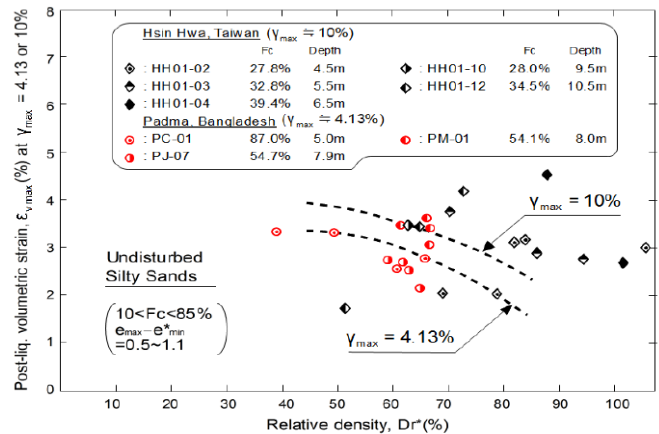
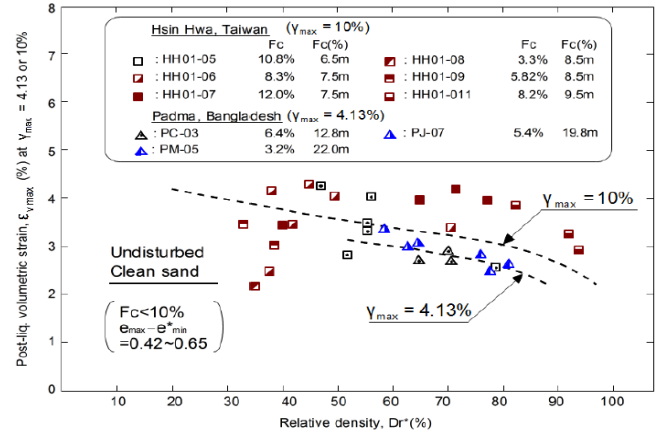


Figure 10 The relationship between relative density and post-liquefaction volumetric strain. (Ishihara et al. 2016)

In summary, current evaluation methods of post-liquefaction settlement are complicated, and the influence of non-plastic silty sand engineering properties on post-liquefaction settlement is not considered. In addition, the influence of disturbance effect is not considered as well. Disturbance effect is the main factor influencing the dynamic properties of non-plastic silty sand. It is different from clean sand; the soil properties of undisturbed non-plastic silty sand specimens are obviously different from that of remolded soil specimens. If no high-quality soil samples can be obtained in the field, the laboratory test results will not represent the true engineering properties of non-plastic silty sand. All test results indicate that the present methods used to evaluate the post-liquefaction settlement of non-plastic silty sand require further improvement. It is anticipated that the results of this study will be used as a reference for engineers prior to designing infrastructure, and for use in liquefaction mitigation works.

3.2 The formulation of current evaluation method

Different from the evaluation method of post-liquefaction settlement proposed by Ishihara & Yoshimine (1992), The chart formulation in this work was initially presented by Chi & Ou (2005), and this research summarizes the evaluation and analysis diagrams of TI&S.2004 by the indoor experimental data and then plots the results. The settlement analysis can only be inquired with the graph, and there is no formula to calculate; thus, it is not easy to analyze the graph when analyzing a large dataset. For convenient calculation, statistical analysis software was used based on the analysis diagram proposed by Tsukamoto et al. (2004) to perform nonlinear regression analysis, and the analytical formula of T.I.&S.2004 was proposed in this study. The two following assumptions about the relationship between the void ratio range ($e_{\max}-e_{\min}$) and volumetric strain normalization value ($\varepsilon_{v\max}/\varepsilon_{vr}$) shown in Figure 9:

1. When the void ratio range is less than 0.5 or greater than 0.7, the volumetric strain normalization value is inversely proportional to the relative density, and the normalization value is a function of relative density where $f(D_r)$ is a single value.
2. When the void ratio range is between 0.5~0.7, $1/(e_{\max}-e_{\min})$ and $\ln(\varepsilon_{v\max}/\varepsilon_{vr})$ have a quadratic linear relationship and are inversely proportional to the relative density.

Based on the two presented assumptions, a regression analysis of the test data was performed by Tsukamoto et al. (2004). Equation (1) representing the relationship between the void ratio range ($e_{\max}-e_{\min}$) and the volumetric strain normalization value ($\varepsilon_{v\max}/\varepsilon_{vr}$) can be expressed as follows:

$$\left(\frac{\varepsilon_{v\max}}{\varepsilon_{vr}}\right) = -0.0027D_r + 0.271 \quad \text{for } (e_{\max}-e_{\min}) \leq 0.5 \quad (1a)$$

$$\left(\frac{\varepsilon_{v\max}}{\varepsilon_{vr}}\right) = e^{\frac{b_1}{(e_{\max}-e_{\min})^2} + \frac{b_2}{(e_{\max}-e_{\min})} + b_3} \quad \text{for } 0.5 < (e_{\max}-e_{\min}) < 0.7 \quad (1b)$$

$$\left(\frac{\varepsilon_{v\max}}{\varepsilon_{vr}}\right) = -0.0041D_r + 0.596 \quad \text{for } (e_{\max}-e_{\min}) \geq 0.7 \quad (1c)$$

Where the undetermined coefficients b_1 ~ b_3 are related to D_r , $b_1 = -0.1499D_r + 4.9092$, $b_2 = 0.4656D_r - 16.216$, and $b_3 = -0.3753D_r + 13.124$. By comparing the calculated results with the original analysis graph, the comparison result is shown in Figure 11. The solid line in the graph represents the analysis curve of the original graph, and the points represent the calculated values obtained by Equation (1). The figure shows the calculation results of the analytical formula derived in this study correspond well with the original analysis chart. In addition, another important analysis

diagram in the TI&S.2004 assessment method is shown in Figure 12, which shows the relationship between the factor of safety (F_L) and $\varepsilon_v/\varepsilon_{v\max}$ proposed by Tsukamoto et al. (2004). The following three characteristics of the curve can be observed:

1. When $\varepsilon_v/\varepsilon_{v\max}$ is equal to 0, the factor of safety is equal to 2 and gradually decreases as $\varepsilon_v/\varepsilon_{v\max}$ increases.
2. When $\varepsilon_v/\varepsilon_{v\max}$ is equal to 0.6, the factor of safety is equal to 1. This point is the inflection point, and the full curve is divided into two segments.
3. When the factor of safety is less than 0.92, $\varepsilon_v/\varepsilon_{v\max}$ approaches 1.

According to the presented three characteristics, the first half of the analysis curve can be confirmed by the trial and error method as the linear relationship of $\ln(\varepsilon_v/\varepsilon_{v\max})$ and $(1/F_L)$, and the latter half of the curve represents the quadratic linear relationship between $(\varepsilon_v/\varepsilon_{v\max})$ and $\ln(F_L)$. The regression analysis was performed using the data of the original curve, and the relationship can be expressed as Equation (2):

$$\left(\frac{\varepsilon_v}{\varepsilon_{v\max}}\right) = e^{\frac{8.5524}{F_L} - 9.1357} \quad \text{for } F_L \geq 1 \quad (2a)$$

$$\left(\frac{\varepsilon_v}{\varepsilon_{v\max}}\right) = -28.157 \ln^2(F_L) - 6.8184 \ln(F_L) + 0.6554 \quad \text{for } 0.92 < F_L < 1 \quad (2b)$$

$$\left(\frac{\varepsilon_v}{\varepsilon_{v\max}}\right) = 1 \quad \text{for } F_L \leq 0.92 \quad (2c)$$

By comparing the calculation result of the above formula with the original analysis graph, the comparison result is shown in Figure 13. The graph shows that the calculation result of the analysis formula deduced in this study corresponds well with the original analysis graph. In summary, the TI&S.2004 method can obtain the factor of safety and relative density of each soil layer from the SPT-N value, and calculate the void ratio range through the fines content and empirical charts. The post-liquefaction settlement calculation steps of the T.I.&S.2004 method are detailed as follows.

Step 1. Calculate the soil liquefaction factor of safety of each soil layer with the SPT-N value.

Step 2. For a known amount of fines content (F_c), the void ratio range ($e_{\max}-e_{\min}$) is estimated through the relation in the following formula:

$$(e_{\max}-e_{\min}) = 0.43 + 0.00867F_c \quad \text{for } F_c < 30\%$$

$$(e_{\max}-e_{\min}) = 0.57 + 0.004F_c \quad \text{for } F_c > 30\%$$

Step 3. Calculate the ε_{vr} with void ratio range ($e_{\max}-e_{\min}$).

$$\varepsilon_{vr} = 29.136(e_{\max}-e_{\min}) + 7.8264$$

Step 4. The N_1 value is calculated by substituting the SPT-N value into the following formula, and the relative density (D_r) of each soil layer is calculated by the void ratio range ($e_{\max}-e_{\min}$) and N_1 value.

$$N_1 = \frac{1.7N}{\sigma'_0 + 0.7}$$

$$D_r = \left[\frac{(e_{\max}-e_{\min})^{1.7}}{9} N_1 \right]^{\frac{1}{2}}$$

Step 5. According to Eq. (1), calculate $\varepsilon_{v\max}$ by the void ratio range ($e_{\max}-e_{\min}$) and ε_{vr} .

Step 6. Substitute the soil liquefaction factor of safety (F_L) and $\varepsilon_{v\max}$ into Eq. (2) to calculate the post-liquefaction volumetric strain, ε_v .

Step 7. Repeat Steps 1~6 to calculate the ε_v of each soil layer and accumulate it downward until the safety factor of liquefied

soil layer is equal to 1.2 to obtain the total subsidence Δs .

$$\Delta s = \sum_{i=1}^N \varepsilon_{v,i} \Delta h_i$$

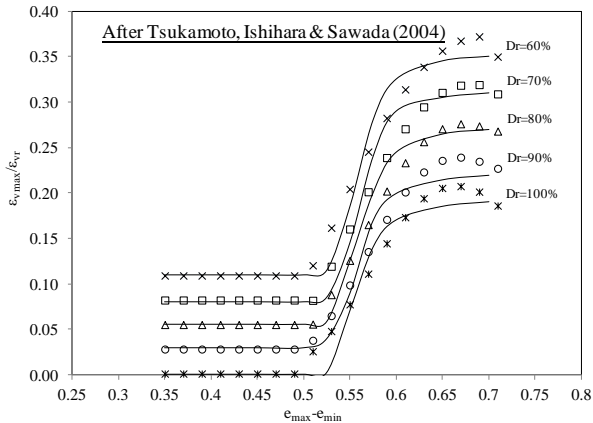


Figure 11 The correspondence between the calculation result of Eq. 1 and the original analysis chart

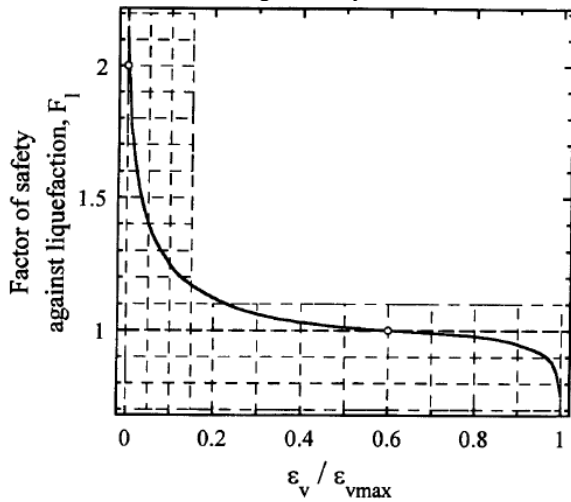


Figure 12 The relationship between normalized post-liquefaction volumetric strain and factor of safety. (Tsukamoto et al., 2004)

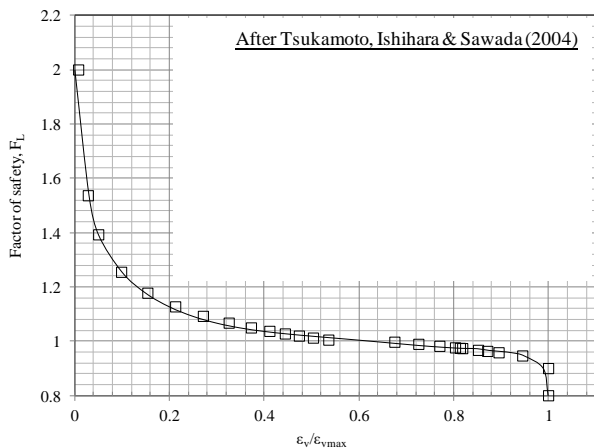


Figure 13 The correspondence between the calculation result of Eq. 2 and the original analysis chart

4. PROPOSED POST-LIQUEFACTION SETTLEMENT ESTIMATION

Two approaches have previously been used to estimate post-liquefaction settlement (volumetric strain). One approach was proposed by Ishihara & Yoshimine in 1992, and chart formulation of this post-liquefaction settlement evaluation method was presented in 2005. The other method was proposed by Tsukamoto, Ishihara,

and Sawada in 2004. These two evaluation methods were based on the soil test results for clean sand or soil with low fines content, and have been constantly applied in related research over the past 10 years. However, earthquakes that have occurred around the world over the past few years have shown that the existence of non-plastic fine aggregate soil reduces soil liquefaction resistance and causes a greater amount of post-liquefaction settlement. Therefore, in this study, we also investigated the applicability of the current post-liquefaction settlement evaluation methods in an area of Taiwan with widespread high fines content.

In this study, we refer to the revised procedure proposed by Ishihara et al. (2016) to suggest modification of the post-liquefaction settlement method and its chart formulation. The Wufeng area was used to verify our modifications, perform calculation analyses, and to discuss results.

4.1 Evaluation method

The current post-liquefaction settlement evaluation methods were proposed based on soil test results for clean sand or soil with low fines content, which is not suitable for non-plastic silty sand layers with high fines content on the southwest coast of Taiwan. To improve the applicability of the current post-liquefaction settlement evaluation methods used in Taiwan, test results of post-liquefaction volumetric strain from non-plastic silty sand specimens were collected in this study, with an aim of proposing suggested modification of the post-liquefaction settlement evaluation method and its chart formulation. Extending the research results proposed by Ishihara et al. (2016), the relationships between post-liquefaction volumetric strain (ε_{vmax}), the void ratio range ($e_{max} - e_{min}$), and relative density (Dr) were further analyzed, as shown in Figures 14 and 15. The soil specimens presented in Figure 15 are grouped according to disturbance state, fines content, and relative density, and the test results of high fines soil contents are divided into four regions by $Dr = 50\%$, 70% , and 90% , as shown in Figure 16. The test results showed the post-liquefaction volumetric strains of remolded soil specimens were significantly larger (by 2 to 2.5 times) than those for undisturbed soil specimens, thereby illustrating that the disturbance effect significantly affects post-liquefaction volumetric strain. There was a decrease in post-liquefaction volumetric strain with an increase in relative density, and an increase in post-liquefaction volumetric strain with an increase in the void ratio range (which is an index parameter used to evaluate the post-liquefaction volumetric strain scale of non-plastic silty sand and can be applied in post-liquefaction settlement evaluation methods). The modified post-liquefaction settlement evaluation method suggests that natural deposition can be analyzed using test results of undisturbed soil specimens, and that post-liquefaction settlement of the artificial backfill area can be analyzed using test results of remolded soil specimens.

To simplify steps used in analysis and the tests conducted using the modified method in this study; test results obtained in the Hsinhwa area were compared with those proposed by Cubrinovski & Ishihara (2002). This confirmed that the analytical charts had the same trends, and therefore, the series of analysis charts and evaluation procedures were utilized for modified post-liquefaction settlement evaluation in Taiwan. Detailed analysis steps used in the modified method are as follows:

Step 1. Given an N -value at each depth at the site under consideration, values for F_L and N_1 are obtained using the normal procedure. For a known amount of fines content (FC), the void ratio range ($e_{max} - e_{min}$) is estimated through the relation in the following formula (Cubrinovski & Ishihara, 2002):

$$(e_{max} - e_{min}) = 0.43 + 0.00867FC \quad \text{for } FC < 30\%$$

$$(e_{max} - e_{min}) = 0.57 + 0.004FC \quad \text{for } FC > 30\%$$

Step 2. The void ratio range ($e_{max} - e_{min}$) and N_1 obtained in Step 1 are substituted into the following equation (Cubrinovski &

Ishihara, 2002) to calculate the relative density (D_r) of each soil layer.

$$D_r = \sqrt{\frac{N_i(e_{\max} - e_{\min})^{1.7}}{9}}$$

- Step 3. When the values of $e_{\max} - e_{\min}$ and D_r are known, the maximum post-liquefaction volumetric strain ($\epsilon_{v\max}$) is estimated using the curves shown in Figure 16.
- Step 4. To enter the factor of safety (F_L) and the maximum post-liquefaction volumetric strain ($\epsilon_{v\max}$) into the chart in Figure 12 (Tsukamoto et al., 2004), the post-liquefaction volumetric strain (ϵ_v) of each soil layer is estimated.
- Step 5. By stepwise integrating volumetric strain (ϵ_v) upward from the conceivable bottom of a liquefiable layer, ground surface settlement is determined. The volumetric strain of each soil layer is multiplied by the thickness of each layer and accumulated, but the settlement of $F_L \geq 1.5$ layer needs to be excluded. The total post-liquefaction settlement of the drilling hole is estimated.

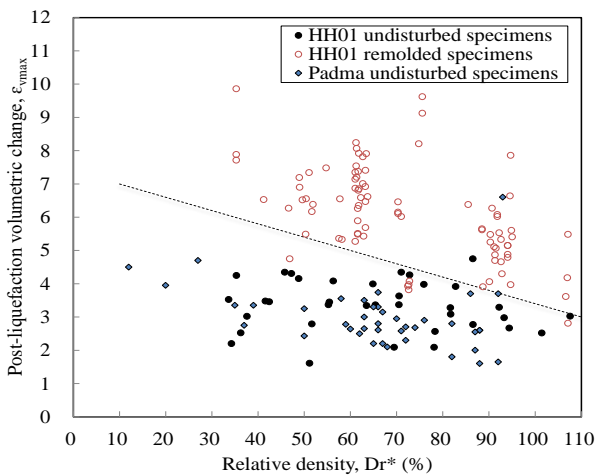


Figure 14 The relationship between post-liquefaction volumetric strain and relative density of silty sand.

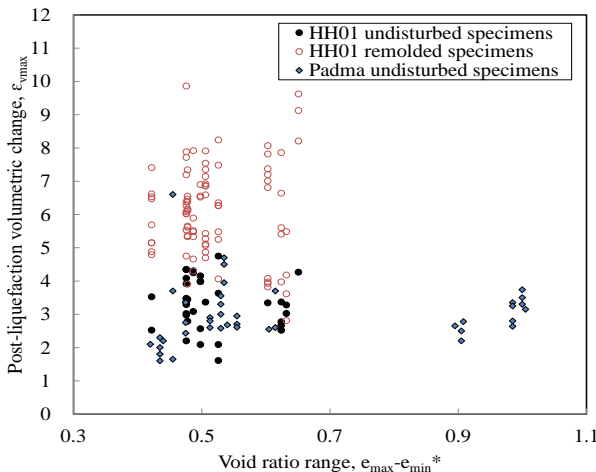


Figure 15 The relationship between post-liquefaction volumetric strain and void ratio range of silty sand.

The analysis procedure used in the suggested modified method for evaluating post-liquefaction settlement is shown in Figure 17. This evaluation procedure was proposed based on test results of dynamic triaxial tests. In the experiment, soil specimens were tested until liquefaction failure occurred, where the volumetric strain after liquefaction was the maximum post-liquefaction volumetric strain ($\epsilon_{v\max}$). However, in actual application, post-liquefaction volumetric strain was found to be related to the soil liquefaction factor of safety (F_L). Therefore, the method provided in Figure 12 should be used to calculate the estimated value of the post-liquefaction settlement (ϵ_v)

under this soil liquefaction factor of safety.

The post-liquefaction settlement evaluation method proposed in this study was revised from that of Ishihara et al. (2016). In the Ishihara et al. (2016) method, the main evaluation concept is based on the relationship between relative density (D_r) and post-liquefaction volumetric strain, but in the current study, the relationship between void ratio range ($e_{\max} - e_{\min}$) and post-liquefaction volumetric strain is found to be more important. Therefore, results of these two evaluation methods clearly differ.

4.2 Case verification

The effect of the Chi-Chi earthquake in the Wufeng area is used to verify the method presented in this study. Excluding drill holes that provided insufficient data, 19 boreholes were used as main verification targets. However, measurement work was not conducted at the drilling site due to subsidence, and the in-situ measured value of surface subsidence in the Wufeng area under the influence of Chi-Chi earthquake determined by Lin (2006) was used as the observed settlement values. A comparison of the observed settlement measured using in-situ work and estimated settlement calculated by our modified evaluation method is shown as follows. The Wufeng area is located in an old sedimentary stratum where non-plastic silty sand is distributed; therefore, post-liquefaction settlement was evaluated using an undisturbed analysis mode. A comparison of analysis results of I&Y1992, T.I.&S.2004, and Ishihara et al. (2016) are shown in Figure 18. The red square in the figure represents the estimated settlement calculated using our modified post-liquefaction settlement evaluation method, and the hollow point is the estimated settlement calculated using the original NJRA method. Furthermore, analysis results from representative boreholes are shown in Figures 19–21.

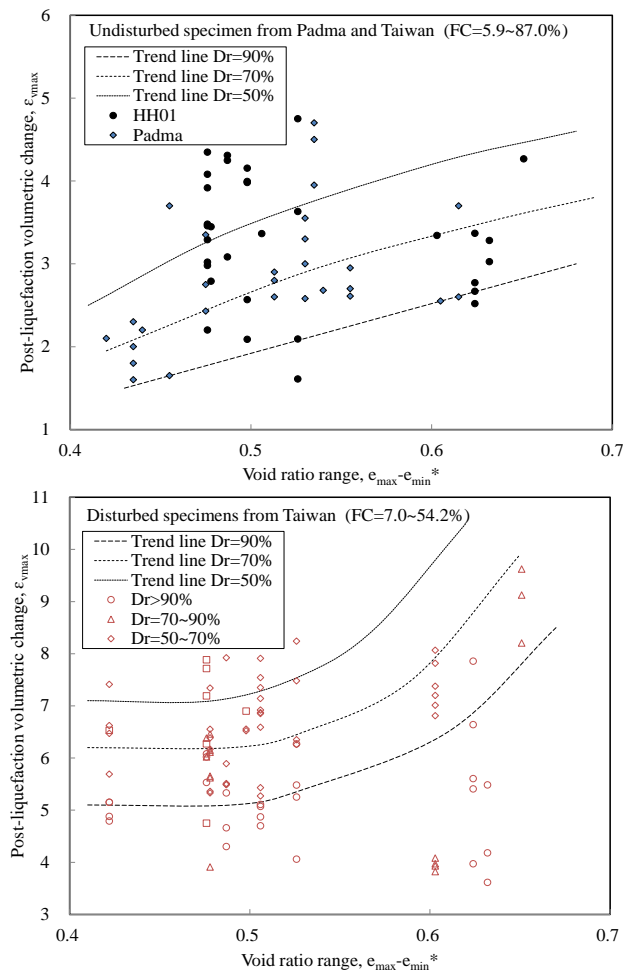


Figure 16 The relationship between post-liquefaction volumetric strain, void ratio range and relative density of Hsinhwa specimens.

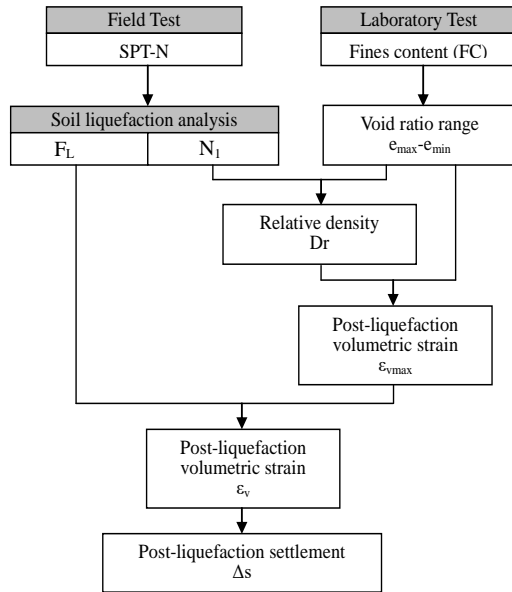


Figure 17 The analysis flow chart of suggested modification on post-liquefaction settlement evaluation method.

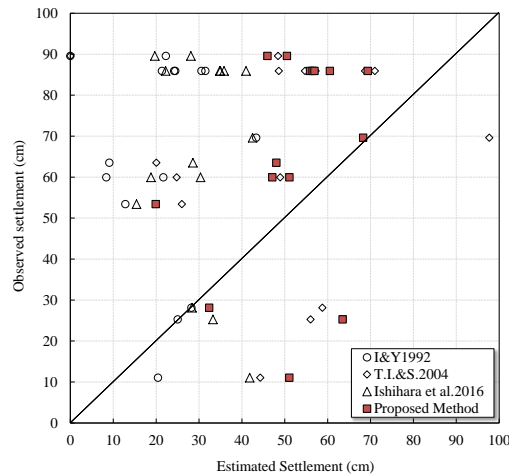


Figure 18 Analysis result comparison of post-liquefaction settlement in Wufeng area.

A comparison of the analysis results of these evaluation methods shown in the figures indicates that the suggested modification method delivers a superior performance in the evaluation of post-liquefaction settlement. I&Y1992 generally underestimated post-liquefaction settlement, whereas T.I.&S.2004 overestimated it. Although the analysis results of Ishihara et al. 2016 are close to those of observed settlement, the analysis results of the suggested modification proposed in this study are more consistent than those of the other method. Previous post-liquefaction settlement evaluation methods were proposed based on soil test results of clean sand (such as I&Y1992 and T.I.&S.2004), and the influence of fine aggregates was often overlooked. However, it is now evident that the fines content has an important effect on post-liquefaction volumetric strain. Furthermore, previous methods frequently identified soil fine aggregates as clayey particles, whereas soil fine aggregates should be divided into two categories, i.e., plastic and non-plastic, where the mechanical properties of both categories differ completely. The disturbance effects can significantly affect analysis results of post-liquefaction volumetric strain, and it is, therefore, necessary to prudently select the appropriate analysis mode. Misjudgements of the influence of non-plastic silty sand on soil liquefaction strength have caused assessment errors of post-liquefaction settlement. The suggested modified method for evaluating post-liquefaction settlement proposed by this study encompasses the abovementioned issues, and thus provides a superior method of evaluations.

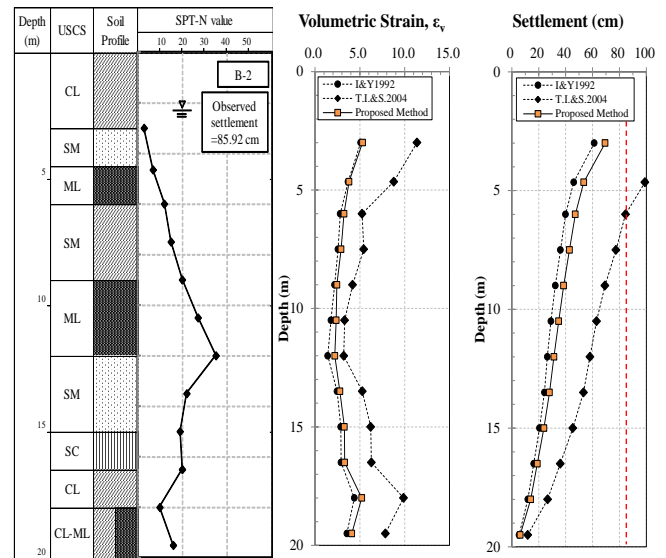


Figure 19 Analysis result of drilling B-2 on post-liquefaction settlement in Wufeng area.

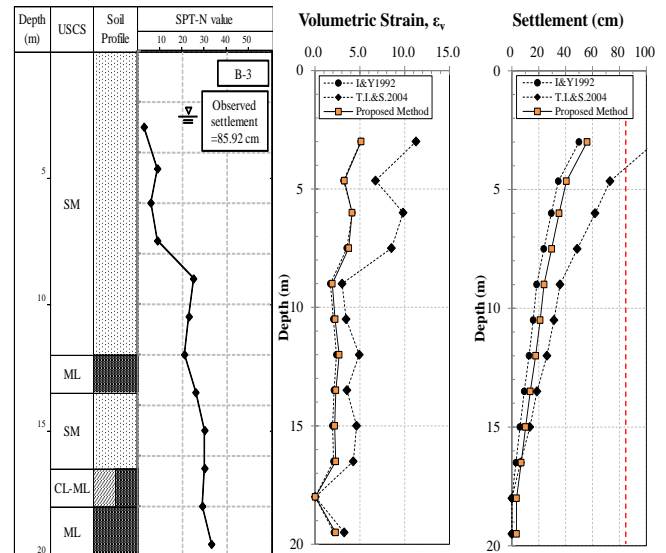


Figure 20 Analysis result of drilling B-3 on post-liquefaction settlement in Wufeng area.

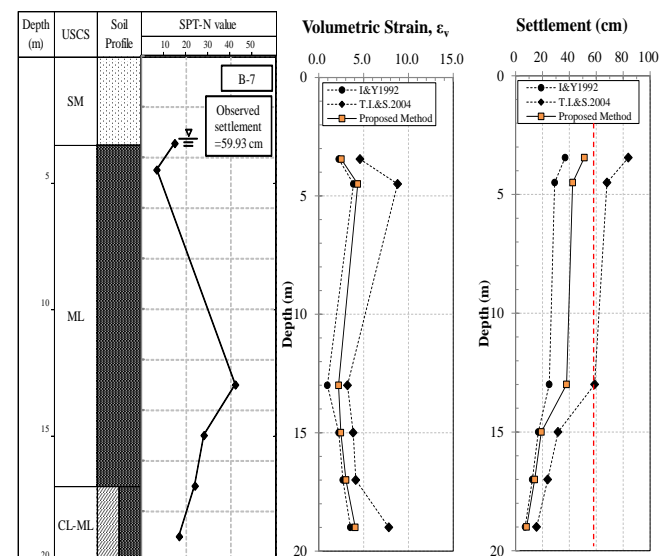


Figure 21 Analysis result of drilling B-7 on post-liquefaction settlement in Wufeng area.

5. CONCLUSION

This study is the first to extend and apply results of research conducted on undisturbed non-plastic silty sand. In this study, high quality undisturbed soil specimens obtained from the Hsinhwa area were used in laboratory tests to investigate the post-liquefaction volumetric strain behavior of non-plastic silty sand, which was found to increase with an increase in the void ratio, the fines content, and the disturbance effect. Additionally, non-plastic silty sand is found to be sensitive and susceptible to soil disturbance. The definition and judgment of disturbance degrees on non-plastic silty sand are pivotal in its post-liquefaction volumetric strain behavior. Previous evaluation methods for post-liquefaction settlement were based on the test results of clean sand, whereas this study is based on silty sand with a high fine content and provides simpler analytical procedures and related application charts. The application of this method is found to be superior to the current methods used. It is necessary only to increase the use of maximum and minimum void ratio tests in practical applications to effortlessly calculate post-liquefaction settlement.

The influence of the fine aggregates has often been overlooked in past post-liquefaction settlement evaluation methods. In actual situations, the fines content and its plasticity are important factors influencing post-liquefaction volumetric strain. Additionally, the disturbance effect should be acknowledged and cannot be ignored. In this respect, when conducting post-liquefaction settlement evaluations, the soil structure and engineering properties need to be firstly understood. In addition, the deposition history of the soil layer also needs to be clarified to select the appropriate assessment analysis mode.

As the suggested evaluation method proposed in this study used only a limited number of test specimens to obtain preliminary results, it is thus suggested that its applicability should be further validated using a greater number of relevant soil tests to enable refinement of the method and further propose methods of evaluating post-liquefaction settlement that is more comprehensive. In addition, this study suggests that detailed soil tests should be conducted both indoors and outdoors to ensure that the true engineering properties of the soil layers are understood prior to building construction. To avoid unnecessary disasters related to any blind spots in this new evaluation method, it is advised that analysis results should not be solely relied on.

6. NOMENCLATURE

CSR	cyclic stress ratio
CSR ₂₀	cyclic stress ratio with number of cycle equal to 20
D ₅₀	average grain size
DA	double amplitude
D _r	relative density
e	void ratio
e _{max} -e _{min}	void ratio range
F _C	fines content
LL	liquid limit,
(N ₁) ₆₀	corrected standard penetration test value
N _c	number of cycle
P _G	plastic grain content
γ _{max}	maximum shear strain
ε _{dmax}	maximum axial strain
ε _v	post-liquefaction volumetric strain
ε _{vmax}	maximum post-liquefaction volumetric strain
ω	moisture content

7. REFERENCES

- Chang, M. H., Chen, J. W., Lee, W. F. (2017) "Post-liquefaction Volumetric Strain Behavior of Non-plastic Silty Sand- a Case Study of Hsin-Hwa Liquefaction", *Journal of Applied Science and Engineering*, Vol. 20, No. 1, pp63-72.
- Chen, C. C., Lee, W. F., Chen, J. W., Ishihara, K. (2014) "Liquefaction Potential of Non-plastic Silty Sand", *Journal of Marine Science and Technology*, Vol. 22, No. 2, pp37-145.
- Chi, Y. Y., Ou, L. T. (2005) "921 Earthquake-Induced Post-Liquefaction Settlement in Yuanlin Area", *Journal of the Chinese Institute of Civil and Hydraulic Engineering*, Vol. 17, No. 4, pp567-576.
- Cubrinovski, M., and Ishihara, K. (2002) "Maximum and Minimum Void Ratio Characteristics of Sands", *Soils and Foundations*, Vol. 42, No. 6, pp65-78.
- Glaser, S. (1993) "Estimating in Situ Liquefaction Potential and Permanent Ground Displacements Due to Liquefaction for the Siting of Lifeline", *National Institute of Standards and Technology*, NISTIR5150.
- Ishihara, K., and Yoshimine, M. (1992) "Evaluation of Settlement in Sand Deposits Following Shear Loading", *Soils and Foundations*, Vol. 32, No. 1, pp173-188.
- Ishihara, K. (1993) "Liquefaction and Flow Failure during Earthquakes", *Geotechnique*, Vol.43, No.3, pp351-415.
- Ishihara, K., Harada, K., Lee, W. F., Chan, C. C., and A. M. M. (2016) "Post-Liquefaction Settlement Analyses Based on the Volume Change Characteristics of Undisturbed and Reconstituted Samples", *Soils and Foundations*, Vol. 56, No. 3, pp533-546.
- Lade, P. V., and Yamamuro, J. A. (1997) "Effects of non-plastic fines on static liquefaction of sands", *Can. Geotech. J.*, Ottawa, 34(6), pp918-928.
- Lee, K., and Albraisa, A. (1974) "Earthquake-Induced Settlements in Saturated Sands", *Journal of Geotechnical Engineering Division, ASCE*, Vol.100, GT4, pp387-405.
- Lee, W. F., Chen, C. C., Chang, M. H., Ge, L. Y. N. (2015) "A Case Study on Silty Sand Liquefaction-2010 Hsin Hwa Liquefaction in Taiwan", In *Perspectives on Earthquake Geotechnical Engineering*, Springer International Publishing, Vol. 37, pp391-414.
- Lin, C. C. (2006) "A Study of Soil Liquefaction-Induced Ground Settlement in Wufeng", Thesis, Department of Civil Engineering, National Chung Hsing University.
- Nagase, H., and Ishihara, K. (1988) "Liquefaction-Induced Compaction and Settlement of Sand During Earthquakes", *Soils and Foundations*, Vol. 28, No. 1, pp65-76.
- Tatsuoka, F., T. Sasaki, and S. Yamada (1984) "Settlement in Saturated Sand Induced by Cyclic Undrained Simple Shear", *Eighth World Conference on Earthquake Engineering*, Vol. 3, pp95-102.
- Tokimatsu, K., and Sees, H. B. (1987) "Evaluation of Settlement in Sands Due to Earthquake Shaking", *Journal of Geotechnical Engineering Division, ASCE*, 113, GT8, pp861-878.
- Tsukamoto, Y., Ishihara, K., and Sawada, S. (2004) "Settlement of silty sand deposits following liquefaction during earthquakes", *Soils and Foundations*, Vol. 44, No. 5, pp135-148.
- Yamamuro, J. A., and Lade, P. V. (1997) "Static liquefaction of very loose sands", *Can. Geotech. J.*, Ottawa, 34(6), pp905-17.
- Yamamuro, J. A., and Lade, P. V. (1998) "Steady-state concepts and static liquefaction of silty sands", *J. Geotech. And Geoenvironmental Engrg.*, ASCE, 124(9), pp868-877.